Social Cognitive and Affective Neuroscience, 2019, 97–107

doi: 10.1093/scan/nsy105
Advance Access Publication Date: 27 November 2018
Original article

Increased functional coupling of the left amygdala and medial prefrontal cortex during the perception of communicative point-light stimuli

Imme C Zillekens,[1,2] Marie-Luise Brandi,[1] Juha M Lahnakoski,[1] Atesh Koul,[4] Valeria Manera,[5] Cristina Becchio,[4,6] and Leonhard Schilbach[1,2,3]

[1]Independent Max Planck Research Group for Social Neuroscience, Max Planck Institute of Psychiatry, 80804 Munich, Germany, [2]International Max Planck Research School for Translational Psychiatry, 80804 Munich, Germany, [3]Department of Psychiatry, Ludwig-Maximilians-Universität, 80539 Munich, Germany, [4]Cognition, Motion and Neuroscience Unit, Fondazione Istituto Italiano di Tecnologia, 16152 Genoa, Italy, [5]CoBTeK Laboratory, Université Cote d'Azur, 06100 Nice, France, and [6]Department of Psychology, University of Turin, 10124 Turin, Italy

Correspondence should be addressed to Imme C Zillekens, Max Planck Institute of Psychiatry, Kraepelinstr. 2-10, Munich 80804, Germany.
E-mail: imme_zillekens@psych.mpg.de.

Abstract

Interpersonal predictive coding (IPPC) describes the behavioral phenomenon whereby seeing a communicative rather than an individual action helps to discern a masked second agent. As little is known, yet, about the neural correlates of IPPC, we conducted a functional magnetic resonance imaging study in a group of 27 healthy participants using point-light displays of moving agents embedded in distractors. We discovered that seeing communicative compared to individual actions was associated with higher activation of right superior frontal gyrus, whereas the reversed contrast elicited increased neural activation in an action observation network that was activated during all trials. Our findings, therefore, potentially indicate the formation of action predictions and a reduced demand for executive control in response to communicative actions. Further, in a regression analysis, we revealed that increased perceptual sensitivity was associated with a deactivation of the left amygdala during the perceptual task. A consecutive psychophysiological interaction analysis showed increased connectivity of the amygdala with medial prefrontal cortex in the context of communicative compared to individual actions. Thus, whereas increased amygdala signaling might interfere with task-relevant processes, increased co-activation of the amygdala and the medial prefrontal cortex in a communicative context might represent the integration of mentalizing computations.

Key words: interpersonal predictive coding (IPPC); point-light displays; fMRI; action observation network; mentalizing

Introduction

Making sense of non-verbal cues constitutes a key requisite to successfully navigate our everyday social interactions. Non-verbal cues allow us to not only deduce valuable information about the intentions of another person, but also to anticipate an appropriate response behavior (Becchio *et al.*, 2012; Sapey-Triomphe *et al.*, 2016). Offering excellent experimental control (Pavlova, 2012), point-light displays of human motion have

Received: 31 January 2018; **Revised:** 2 November 2018; **Accepted:** 21 November 2018

frequently been used to investigate the perception of non-verbal cues (Neri *et al*., 2006; Marsh *et al*., 2009). Numerous studies demonstrated that kinematic information derived from point-light displays can reliably be used to infer the intentions of an actor, consequently facilitating the visual detection of a second agent that responds to a communicative action shown by the first agent (Saygin *et al*., 2004; Manera *et al*., 2010, 2011a; Becchio *et al*., 2012). The underlying phenomenon has been described as interpersonal predictive coding (IPPC; Manera *et al*., 2013; von der Lühe *et al*., 2016) and refers to the Bayesian account of the brain as a 'prediction machine' that uses an internal model to generate hypotheses, so-called priors, about the external world (Friston, 2002). While perception relies on a combination of sensory input and priors, the underlying internal models are constantly updated to account for deviating sensory input, namely, the so-called prediction error. Importantly, the Bayesian account assumes that the more ambiguous a sensory environment, the more does the organism rely on prior top–down expectations that drive perception and minimize the prediction error. For instance, a communicative action of an agent might increase perceptual sensitivity in a noisy environment as the sensory input can be compared with a concrete hypothesis about a second agent (prior), facilitating the detection of this second agent (Manera *et al*., 2011b). Strikingly, the behavioral effect of IPPC of increased sensitivity to discriminate between presence and absence of a second agent was not found in individuals with high-functioning autism, a psychiatric condition that is characterized by impairments in communication and social interaction (von der Lühe *et al*., 2016).

Despite a growing number of behavioral studies (Manera *et al*., 2011b; von der Lühe *et al*., 2016; Okruszek *et al*., 2017), the neural correlates of IPPC remain elusive. To address this empirical gap, we adapted the paradigm applied by Manera and colleagues (Manera *et al*., 2011b, 2011c) for neuroimaging purposes. Participants observed point-light agents either performing a communicative or an individual action and were asked to indicate as fast as possible via button press whether a neighboring cloud of dots contained a second agent (Signal) or not (Noise). Our dependent variables were derived from 'signal detection theory' (Stanislaw and Todorov, 1999). We analyzed the sensitivity to discriminate between presence and absence of the second agent, expressed by d' and evaluated the tendency to select one response category (presence) over the other (absence), captured by response criterion c (s. equations 1 and 2). In a behavioral study, we validated the modified paradigm by replicating the enhancing effect of communicative actions on sensitivity d' (cf. Manera *et al*., 2011b; von der Lühe *et al*., 2016). Based on previous results Manera, *et al*., (2011c), we hypothesized participants to be more likely to perceive a second agent after communicative compared to individual actions, which would be expressed by a decreased criterion c in communicative trials. Subsequently, we applied the paradigm in a functional magnetic resonance imaging (fMRI) study to investigate the neural correlates of IPPC. First, to gain a general impression of neural processing during our paradigm, we contrasted activation during task over all experimental conditions against the blood oxygenation level dependent (BOLD) signal in our implicit baseline. Expecting to find regions involved in action observation and biological motion processing such as dorsolateral motor, superior parietal, posterior temporal and visual areas (Caspers *et al*., 2010; Pavlova, 2012), we next analyzed the specific effects of communicative and individual actions on neural signaling. Representing socially interactive and hence, predictive stimuli, we anticipated communicative contrary to individual actions to evoke an increased BOLD response in core areas of the so-called 'social brain' such as medial prefrontal and orbitofrontal cortex, which have been linked to the attribution of intentions, dynamic social perception (Amodio and Frith, 2006; Yang *et al*., 2015) as well as the processing of frequent and predictable event sequences (Wood *et al*., 2004). We additionally evaluated the BOLD response to non-predictive, individual actions and the interaction of experimental conditions by contrasting non-expected trial outcomes (Noise after communicative actions and Signal after individual actions) to expected trial outcomes (Signal after communicative actions and Noise after individual actions). Moreover, we were interested in the brain correlates of the two 'signal detection theory' parameters d' and c. Although van Kemenade *et al*. (2012) measured a reduction in sensitivity to biological motion and a shift in response criterion toward positive responses after repetitive transcranial magnetic current stimulation over the premotor cortex, the neural correlates of perceptual discriminability and response tendencies rest largely unknown, particularly in a paradigm of predictive and non-predictive action cues potentially recruiting higher-order neural computations (van Pelt *et al*., 2016). Thus, in our study, we correlated the participants' sensitivity d' and criterion c values with neural activation during the task compared to baseline. Observing that neural activity in the amygdala was negatively associated with d', we consequently conducted a psychophysiological interaction analysis to further assess how the connectivity of the amygdala is modulated by the communicative as compared to the individual context.

Methods

Participants

Of the 21 healthy volunteers in the behavioral validation study, 2 participants were excluded from the analysis as their performance did not significantly exceed chance level (Mueller-Putz *et al*., 2008). Responses of another participant could not be recorded. Of the remaining 18 participants, 9 were female. The age ranged between 20 and 29 years (M = 23.22, s.d. = 2.76). In the fMRI study, caused by the temporal constraints and difficulty of the paradigm, which had the purpose of triggering false positive (FA) responses, 9 out of 50 participants did not achieve a performance above chance level. Due to missing data, two data sets were lost. Furthermore, nine participants did not fulfill the requirements of the fMRI analysis ($\geq$16 valid trials in each combination of condition). We additionally excluded two participants who showed repeated translational motion (>3 mm) as well as neural signal loss due to susceptibility artifacts. In one participant, an anatomical screening procedure revealed abnormalities. Thus, the final sample of the fMRI study comprised 13 female and 14 male participants, aged 20–50 years (M = 26.63, s.d. = 6.55). All participants of both the behavioral and the fMRI study were right-handed (Oldfield, 1971), had normal or corrected to normal vision and no history of neurologic or psychiatric illness. Independent of the performance in the task, participants received a monetary compensation of 10€ per hour. The experimental procedures followed the guidelines of the Declaration of Helsinki and were approved by the ethics committee of the Ludwig-Maximilians-Universität München.

Experimental design

In the present study, we used an adapted version of a previously published yes–no paradigm (Manera *et al*., 2011c). Using Psychophysics Toolbox (Version 3.0.11.: Brainard, 1997;

Table 1. Experimental conditions. Actions of agent A define communicative (COM) and individual (IND) trials, whereas the presence or absence of agent B defines trials as Signal or Noise trials, respectively. Given the combination of a communicative action of agent A and the presence of agent B (COM and Signal), agent B's response action corresponds to the communicative action of agent A.

Agent A		*Agent B*	
Communicative (COM)	**Individual (IND)**	**Signal**	**Noise**
Asking to squat down	Turning around	Squatting down	Absent
Asking to look at the ceiling	Sneezing	Looking at the ceiling	Absent
Asking to sit down	Drinking	Sitting down	Absent

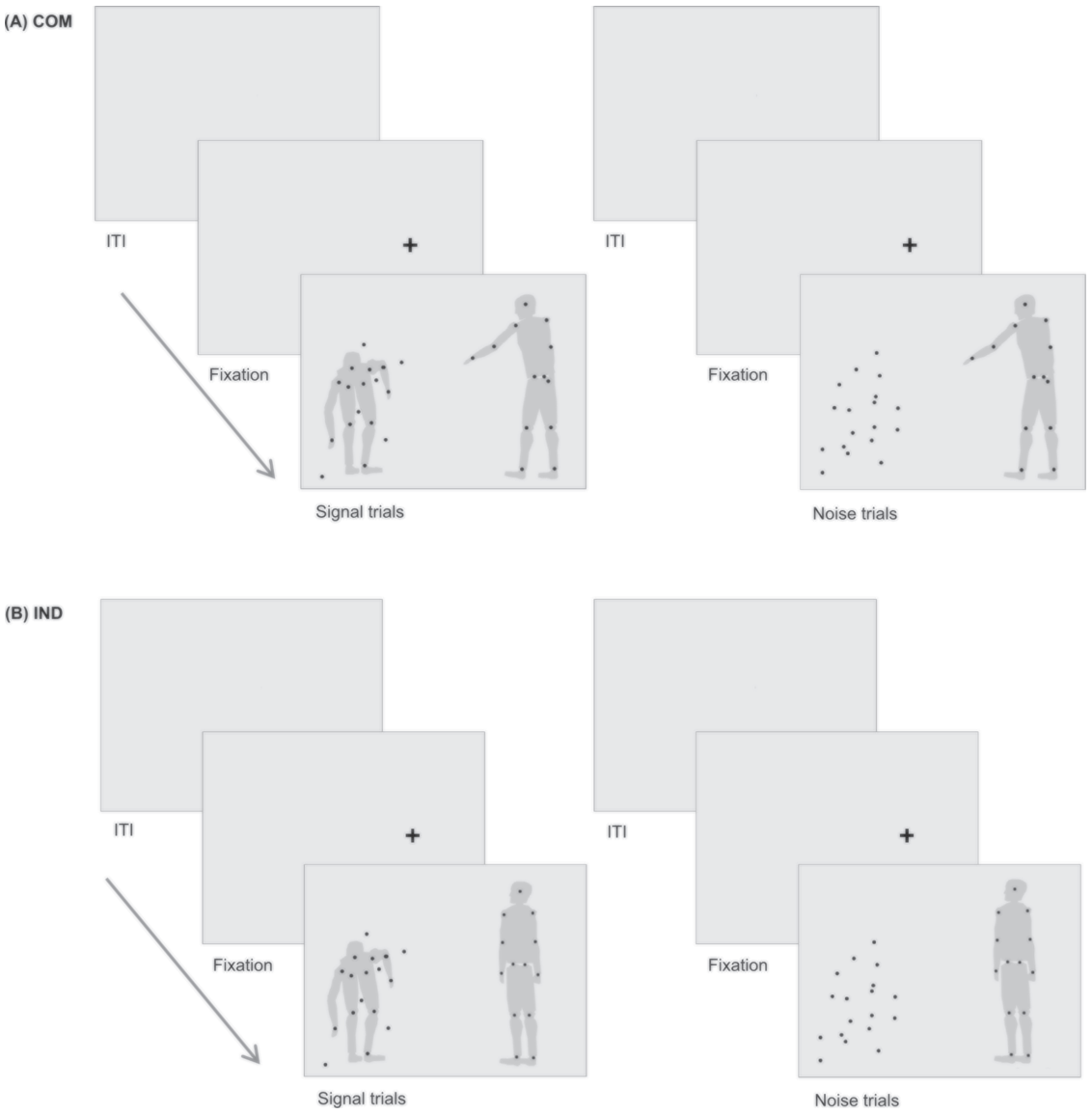

Fig. 1. Structure of experimental trials. Jittered ITIs preceded a fixation cross appearing at the subsequent position of agent A. Participants were asked to first, look at agent A, second, fixate the cloud of dots and third, indicate the presence (Signal) or absence (Noise) of agent B via a button press. (A) depicts trials of the communicative condition (COM); (B) exemplifies the individual condition (IND). On the left, agent B is present (Signal trial), reacting in accordance to the communicative action of agent A. On the right, agent B is replaced by randomly moving noise dots (Noise trial). The gray silhouettes serve illustrative purposes and were not visible for participants.

Kleiner *et al.*, 2007) in Matlab R2015a (The MathWorks, Inc., Natick, Massachusetts, USA), we presented black moving dots on a gray background. On one side of the computer monitor (refresh rate = 59 Hz, resolution of 1024 × 768, viewable region of 375 × 280 mm), moving dots constituted an agent (agent A), who performed a communicative (COM) or an individual (IND) action (Table 1). On the other side of the screen, a cloud of temporally and spatially scrambled moving dots was displayed (for details, see Manera *et al.*, 2011c). In 50% of trials, a second agent (agent B) was present within the cloud and reacted to the action of agent A (Signal trials); in the remaining 50% of trials, the dots' motion was scrambled (Noise trials; Figure 1). From this 2 (type of action) × 2 (type of trial) design we obtained four experimental conditions: COM_Signal, COM_Noise, IND_Signal

and IND_Noise. Although being presented simultaneously, agent B's action always succeeded agent A's action without any temporal delay. Movements of the agents were chosen from the Communicative Interaction Database and have been shown to be reliably recognizable (Manera *et al*., 2010, 2011c). Stimulus duration ranged from 2885 to 3473 ms and the distance from the center of the screen was comparable between actions. To avoid participants' reliance on simultaneous transitions of dots defining agent B's body, we applied a so-called limited lifetime technique (Burr *et al*., 1998; Neri *et al*., 2006). Of 13 possible positions constituting agent B, only 6 were occupied by Signal dots at a given time. The 'lifetime' of the dots was limited because after 200 ms, a dot disappeared and reappeared at another position. Desynchronized timing of dot appearance further prevented joint transitions of stimuli. The position of agents on the left or right side of the screen was counterbalanced.

Procedure

Participants either took part in the behavioral or the fMRI study. After providing written informed consent, they completed a pretest and the main part of the experiment. The pretest consisted of 108 trials and served at defining the individual level of noise dots to be employed. For this purpose, we presented the cloud of dots potentially containing agent B, and manipulated the difficulty in the task of correctly indicating the presence or absence of agent B by employing a cloud of 5, 20 or 40 dots. Fitting a cumulative Gaussian function to participants' performance, we derived the number of dots corresponding to a performance of 70% correct responses. Pursuing Manera *et al*.'s (2011a, 2011b) procedure, if the estimated number of dots was lower than five, it was set to five. The participant-specific number of noise dots estimated with this procedure was utilized in the main part of the experiment, which consisted of 144 trials in the behavioral study and of 192 trials in the fMRI study. During four example trials, the participant was familiarized with the task. Each trial was preceded by a fixation cross indicating the subsequent position of agent A and followed by a blank screen for a jittered inter-trial-interval (ITI) with mean duration of 2 s (range = 1–3 s) in the behavioral and 4 s (range = 3–5 s) in the fMRI study. The participant was instructed to initially fixate agent A, then look at the cloud of dots and indicate as soon as possible whether agent B was 'present' or 'absent'. Responses could be given as long as stimuli were presented. Across participants, the position of the response buttons [s- or l-key on a standard German (QWERTZ) keyboard or left or right button on a button box in the main part of the fMRI study] was counterbalanced. While completing the task, an eye-tracking camera (EyeLink 1000 Plus; SR Research, Osgoode, ON, Canada) recorded participants' right eye with a sampling rate of 1000 Hz. In the fMRI study, an MRI-compatible version of the same eye-tracking system was used. After a 9-point calibration and validation procedure, the fixation duration on agent A was evaluated online and participants would be shown a warning message if the fixation was shorter than 1000 ms in 3 consecutive trials, sensitizing participants to initially fixate agent A.

Behavioral data analysis

Behavioral data analysis was performed in Matlab R2015a. Effect sizes (Cohen's d_z) cited in this paper represent statistics described in Lakens (2013). For the pre-processing of eye-tracking data, we used the software package edar by Tore Erdmann (https://github.com/toreerdmann/edar; retrieved 26 July 2017) in R (Version 3.3.1, R Foundation, Vienna, Austria).

Fixation durations represented the cumulative duration of all initial fixations over all trials, i.e. static eye positions longer than 100 ms (Version 1.5.0, Eyelink 1000 User Manual) with time points of blinks being removed from the data. If participants fixated each agent for 200 ms or more, i.e. spend at least 200 ms on the side of the screen on which the respective agent or Noise was presented, a trial was declared as 'valid'. We further excluded trials in which a response was given after the stimuli had already disappeared or before fixating agent B (s. Supplementary Table S1 for details). Reaction times (RTs) comprised the time window between the last fixation on agent A and a button press. All subsequent analyses were based on valid trials.

In order to obtain the two 'signal detection theory' parameters sensitivity d' and response criterion c, we calculated the FA rate (proportion of false positive responses of all Noise trials) and hit rate (proportion of true positive responses of all Signal trials). Next, hit and FA rates were z-transformed and employed through the following formulas:

$$d' = Z\,(Hit\ rate) - Z\,(FA\ rate) \tag{1}$$

$$c = -\,(1/2) * \left[Z\,(Hit\ rate) + Z\,(FA\ rate)\right] \tag{2}$$

Testing the assumption that IPPC increases perceptual sensitivity, we compared d' in the communicative to the individual condition by employing paired one-sided t-tests. Using the same statistical analyses, we addressed our expectation of a bias toward responding 'present', i.e. a lower criterion in communicative compared to individual trials. Last, to exclude an association of length of evidence accumulation and perceptual sensitivity, we correlated the fixation duration on agent B/Noise with d'.

fMRI acquisition and data analysis

In the fMRI study, the main part of the experiment took place inside a 3T MR scanner (MR750; GE, Milwaukee, USA). For design efficiency reasons (Henson, 2007), we added 35 null trials of 4 s duration to the design prolonging the ITI and representing our baseline trials. The experiment comprised a single functional run of 791 volumes of 40 slices {32-channel head coil, AC-PC-orientation, 96 × 96 matrix, 3 × 3 mm voxel size, 3 mm slice thickness, 0.5 mm slice gap, echo planar imaging [repetition time (TR) of 2000 ms, echo time (TE) of 20 ms, 90° flip angle]}. By removing the first nine volumes, we controlled for T1 non-equilibrium effects. FMRI data pre-processing and analysis were performed in SPM12 (Statistical Parametric Mapping Software, Wellcome Department of Imaging Neuroscience, London, UK, http://www.fil.ion.ucl.ac.uk/SPM). By the means of rigid body transformation, functional images were spatially realigned to the mean image. After coregistration, images were spatially normalized to the Montreal Neurological Institute (MNI) template using tissue segmentated T1-weighted anatomical images (BRAVO FSPGR pulse sequence, 1 mm isotropic voxels, TR of 6.2 ms, TE of 2.3 ms). Voxels of functional images were resliced to 2 × 2 × 2 mm. For spatial smoothing, we applied a 3D Gaussian Kernel with full width of half maximum of 8 mm. Experimental trials as well as baseline trials were modeled as single epochs of trial duration in a general linear model (GLM) and convolved with a hemodynamic response function. Four regressors accounted for the experimental conditions of trial type (Noise *vs* Signal trial) x type of action [communicative (COM) *vs* individual (IND)]. No

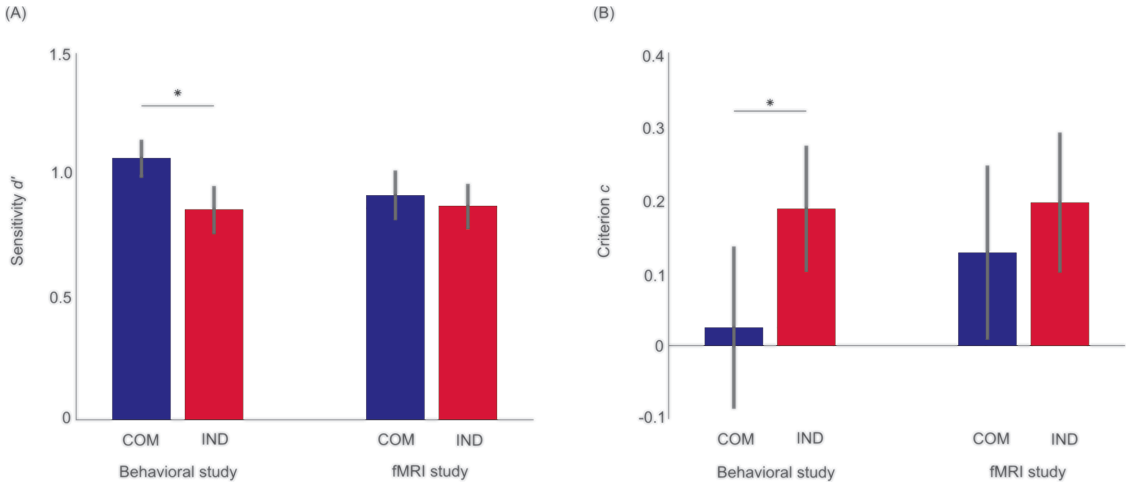

Fig. 2. Effect of IPPC on signal detection theory parameters. (A) Mean sensitivity d' values and (B) mean criterion c values in the communicative (COM) and individual (IND) conditions of the behavioral and the fMRI study. Error bars represent the standard error of the mean (SEM), the asterisks mark statistically significant ($P < 0.05$) differences.

global scaling was applied and low-frequency signal drifts were filtered using a cut-off period of 128 s. Voxel-wise maximum likelihood estimators were estimated thereby considering the temporal autocorrelation of the data (Kiebel and Holmes, 2004). On the first level, we included six motion regressors and two regressors capturing the first principal component of confounding signal from white matter (WM) and cerebrospinal fluid (CSF), which on average accounted for 86% (s.d. = 3%) and 79% (s.d. = 5%) of the variance in the signal from WM and CSF, respectively (Caballero-Gaudes and Reynolds, 2017). For this, we obtained a binarized mask from the respective structural images using a 0.95 threshold in SPM's image calculator (imcalc) and performed a principal component analysis of signals in WM and CSF for each participant. Finally, invalid trials were captured by a regressor of no interest. On the second level, a flexible factorial design was set up, analyzing condition effects on the group BOLD contrast. A subject factor was added to the design and SPM12's default settings of unequal variances over experimental conditions and subjects were implemented. We analyzed the main effect of communicative actions [(COM_Signal + COM_Noise) > (IND_Signal + IND_Noise)] and the reversed contrast of individual actions [(IND_Signal + IND_Noise) > (COM_Signal + COM_Noise)], as well as the main effects of presence [(COM_Signal + IND_Signal) > (COM_Noise + IND_Noise)] and absence of agent B [(COM_Noise + IND_Noise) > (COM_Signal + IND_Signal)]. Calculating experimental interactions of experimental main effects, we included a contrast of expected outcome (EO) [(COM_Signal + IND_Noise) > (IND_Signal + COM_Noise)], i.e. trials including agent B reacting to a communicative action and Noise following individual actions of agent A subtracted by activation during Noise after communicative and Signal after individual actions. Similarly, we calculated the reversed contrast of non-expected outcome (NEO) [(COM_Noise + IND_Signal) > (COM_Signal + IND_Noise)]. Additionally, on the second level, we performed a regression analysis defining sensitivity d' over both conditions as a covariate of interest in a one-sample t-test of task compared to baseline activation and repeated the procedure for criterion c as a covariate of interest. Finally, we explored if and how the functional coupling of the amygdala as a region of negative association with perceptual sensitivity differs between communicative and individual actions. To this end, we conducted a generalized condition-specific psychophysiological interaction analysis (McLaren *et al.*, 2012). ROI (region of interest) coordinates were derived from Neurosynth [Yarkoni *et al.*, 2011; (−22 −4 −18); term = 'Amygdala'; zscore = 33.11; retrieved 12 September 2017, from www.neurosynth.org] and ROI spheres of 6 mm radius were created with marsbar toolbox (Brett *et al.*, 2002). We extracted the eigenvariate and allowed actual ROIs to vary in size between participants ('equalroi' = 0) but restricted them to first-level masks generated by SPM12 to find brain correlates in the context of communicative compared to individual actions and vice versa. Statistical maps are shown at a cluster forming threshold of $P < 0.005$ (uncorrected) and a cluster threshold of $P < 0.05$ (FWE). Maps of the psychophysiological interaction analysis are presented at a threshold of $P < 0.05$ (FWE) at voxel level and a cluster size of $k > 100$, considering the smoothness of the data. For functional localization we utilized the Anatomy Toolbox (Eickhoff *et al.*, 2005) (Version 2.2c) and applied Surf Ice from (https://www.nitrc.org/projects/surfice/) and MRIcron (Rorden and Brett, 2000) for all brain visualizations.

Results

Behavioral results

The average difficulty in the behavioral experiment was 10.56 (s.d. = 6.20) interfering dots. As intended, participants correctly identified Signal or Noise in 70.53% (s.d. = 6.80%) of valid trials. In comparison, implementing a mean number of 12.19 dots (s.d. = 8.36) in the fMRI experiment, participants achieved a performance of 69% (s.d. = 7.6%) correct responses. Confirming our hypothesis, a paired one-sided t-test attested a significant increase of d' in communicative ($M = 1.34$, s.d. = 0.39) compared to individual trials ($M = 1.08$, s.d. = 0.53) in the behavioral study, $t(17) = 2.30$, $P < 0.05$, $d_z = 0.56$. In the fMRI study, the effect of sensitivity being higher in the communicative ($M = 1.15$, s.d. = 0.61) compared to the individual condition ($M = 1.10$, s.d. = 0.59) remained non-significant, $t(26) = 0.64$, $P = 0.26$ (Figure 2A). Concerning the impact of the type of action on participants' response bias, in the behavioral study, participants were more biased toward reporting the presence of a second agent in communicative ($M = 0.02$, s.d. = 0.47) than in individual

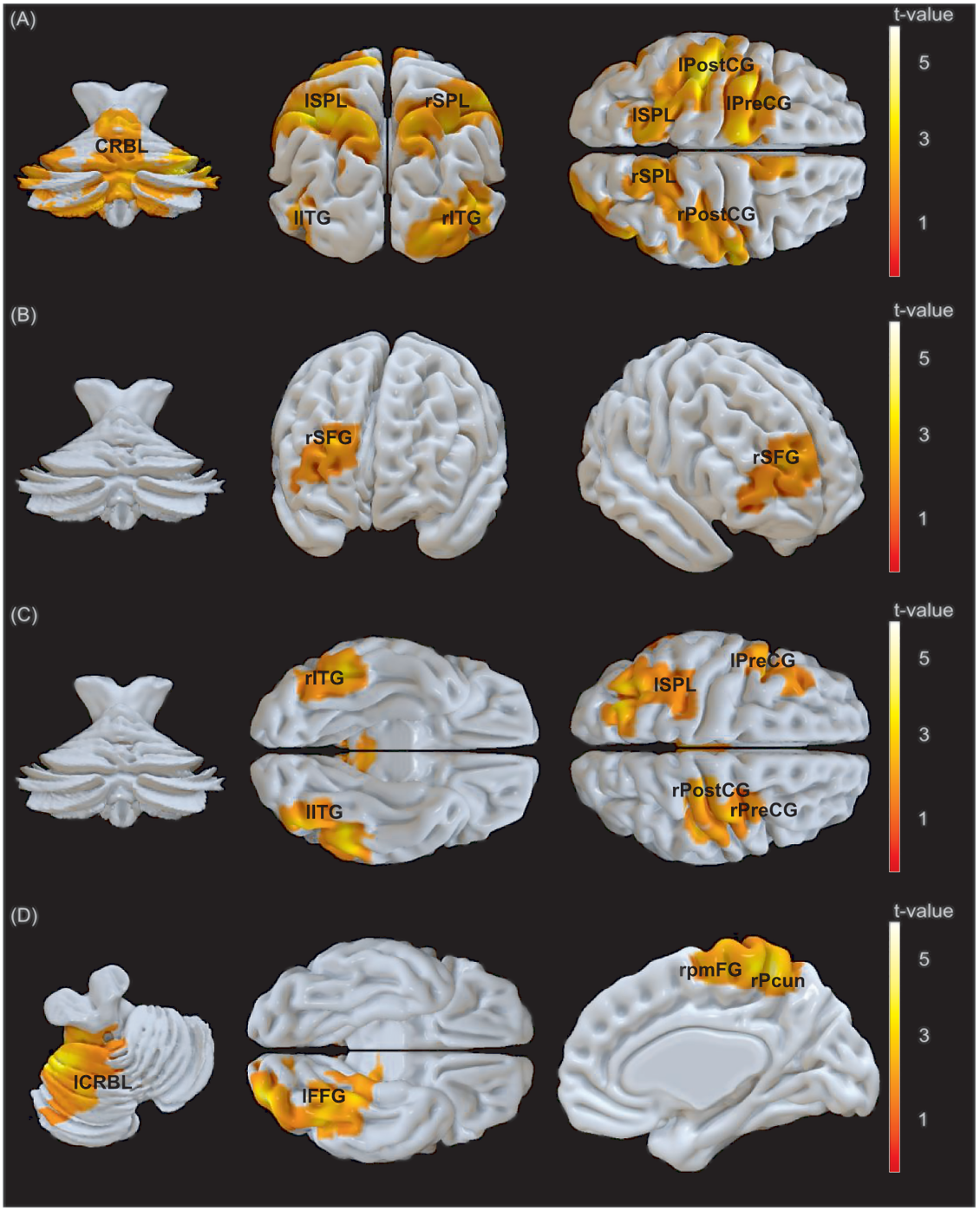

Fig. 3. (A) Clusters of activation of the contrast task greater than baseline, the main contrasts of (B) communicative *vs* individual (COM > IND), (C) individual *vs* communicative (IND > COM) trials and (D) the interaction effect of conditions, depicting the contrast of NEO *vs* EO. The cluster forming threshold was set to $P < 0.005$ (uncorrected), the cluster threshold to $P < 0.05$ (FWE) and cluster size (A) $k > 1026$ voxels, (B) $k > 507$ voxels, (C) $k > 1078$ voxels and (D) $k > 565$ voxels. [(A) CRBL, cerebellum; l/rSPL, left/right superior parietal lobule; l/rITG, left/right inferior temporal gyrus; l/rPostCG, left/right postcentral gyrus; lPreCG, left precentral gyrus; (B) rSFG, right superior frontal gyrus; (C) l/rITG, left/right inferior temporal gyrus; lSPL, left superior parietal lobule; rPostCG, right post-central gyrus; l/rPreCG, left/right pre-central gyrus; (D) lCRBL, left cerebellum; lFFG, left fusiform gyrus; rpmFG, right posterior medial frontal gyrus; rPcun, right precuneus]

trials ($M = 0.19$, s.d. = 0.50), $t(17) = 2.61$, $P < 0.01$, $d_z = 0.63$. Similarly, in the fMRI study, a paired one-sided *t*-test revealed a trend of *c* being lower in the communicative condition ($M = 0.13$, s.d. = 0.44) than for individual actions ($M = 0.20$, s.d. = 0.49), $t(26) = 1.20$, $P = 0.12$ (Figure 2B).

Crucially, d' and *c* were uncorrelated in both studies and could thus be used as independent predictors in our brain–behavior correlation analysis [behavioral: $r(16) = -0.10$, $P = 0.69$; fMRI: $r(25) = 0.16$, $P = 0.44$]. Furthermore, a null correlation between the fixation duration on agent B/Noise and d' in the behavioral

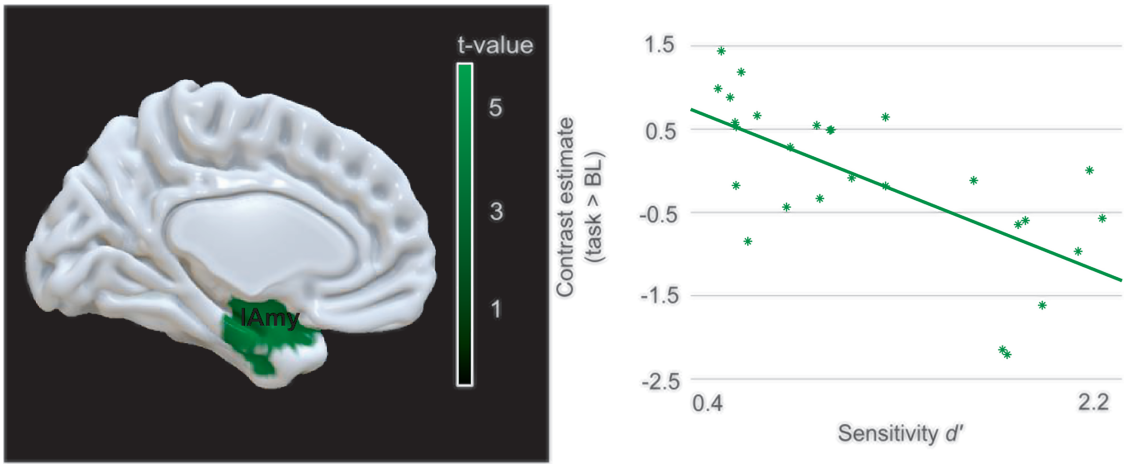

Fig. 4. Task-related brain activity modulated by participants' sensitivity d′. Brain activity map depicting brain regions whose neural activation during task compared to baseline negatively correlated with sensitivity d'. The scatterplot visualizes the relationship of sensitivity d' with the contrast estimates of the respective peak region. The cluster forming threshold was set to $P < 0.005$ (uncorrected), the cluster threshold to $P < 0.05$ (FWE) and cluster size $k > 260$ voxels. [lAmy, left amygdala]

study ruled out that prolonged fixation of the cloud determined participants sensitivity d', $r(16) = -0.03$, $P = 0.90$. Equally, in the fMRI study, fixation duration and sensitivity were uncorrelated $r(25) = 0.12$, $P = 0.55$ (s. Supplementary Tables S2 and S3 for details).

Supplemental paired one-sided *t*-tests were used to investigate condition-specific differences in the sub-components of d' and c, namely the FA and true positive (hit) rates. To correct for multiple comparisons, we Bonferroni corrected the original alpha level of 0.05 for the two independent tests for each sub-component. Results show that the FA rate did not differ between conditions neither in the behavioral [$t(17) = 0.27$, $P = 0.39$] nor the fMRI study [$t(26) = 0.93$, $P = 0.18$]. The hit rate, however, was significantly larger in communicative compared to individual trials in the behavioral study, $t(17) = 2.87$, $P < 0.01$. This pattern emerged as a trend in the fMRI study, $t(26) = 1.68$, $P = 0.053$.

Neural correlates

Task compared to baseline elicited bilateral neural activation in the inferior and superior parietal lobules, post- and the left pre-central gyri, inferior temporal, occipital and cerebellar regions (Figure 3A and Supplementary Table S4). The first main contrast, namely communicative contrasted to individual trials [(COM_Signal + COM_Noise) > (IND_Signal + IND_Noise)], was associated with significantly higher BOLD signal in the right superior frontal gyrus (SFG) (Figure 3B), an effect primarily driven by the contrast of COM_Noise > IND_Signal (Supplementary Figure S1). The reversed contrast [(IND_Signal + IND_Noise) > (COM_Signal + COM_Noise)] was accompanied by an increased BOLD response in the left superior parietal lobule, inferior temporal gyri as well as frontal areas with peaks in the pre-central and the right post-central gyri (Figure 3C). Depicting the interaction effects of experimental conditions, the EO contrast [(COM_Signal + IND_Noise) > (IND_Signal + COM_Noise)] did not evoke any suprathreshold activation, whereas the reversed NEO contrast [(COM_Noise + IND_Signal) > (COM_Signal + IND_Noise)] showed activation in the right posterior medial frontal gyrus (PMFG), bilateral precunei, left cerebellum and left fusiform gyrus (FFG; s. Figure 3D; Supplementary Tables S5 and S6 for all main and interaction effects of experimental conditions).

Brain–behavior correlations

To shed light on the relationship of neural activation and the 'signal detection theory' parameters across subjects and across conditions, sensitivity d' and criterion c values were used as covariates of interest in two separate second-level analyses of activation differences for task compared to baseline. While we did not find a positive correlation, the first analysis showed a negative association of sensitivity d' and activity in a left lateralized cluster in the inferior temporal gyrus including peak activation in the amygdala. In the second regression analysis, we neither identified a significant positive nor negative neural correlate of subject-specific criterion values (Figure 4 and Supplementary Table S7).

Connectivity analysis

A psychophysiological interaction analysis was used to investigate the functional coupling of the left amygdala in the context of communicative and individual actions (Figure 5 and Supplementary Table S8). For individual contrasted to communicative actions (IND_Signal + IND_Noise) > (COM_Signal + COM_Noise), the left amygdala co-activated with a dorsal fronto-parietal network comprising bilateral inferior and superior parietal lobules and the middle frontal gyri, spreading to the pre-central gyri and the left inferior frontal gyrus. Additionally, co-activation was spread over the inferior temporal gyri and cerebellum. In response to communicative compared to individual actions [(COM_Signal + COM_Noise) > (IND_Signal + IND_Noise)], activation in the amygdala was coupled to activation in a prominent bilateral cluster in medial prefrontal cortex (mPFC) consisting of superior medial and orbitofrontal gyri and the right anterior cingulate cortex. Peak co-activation also occurred in the left temporal pole (Tp).

Discussion

In the present study, we used an fMRI-compatible version of an established signal detection task to investigate the behavioral and neural correlates of IPPC. We replicated the behavioral finding of higher sensitivity and less conservative response criteria in communicative compared to individual actions and demonstrated that this effect was driven by a higher proba-

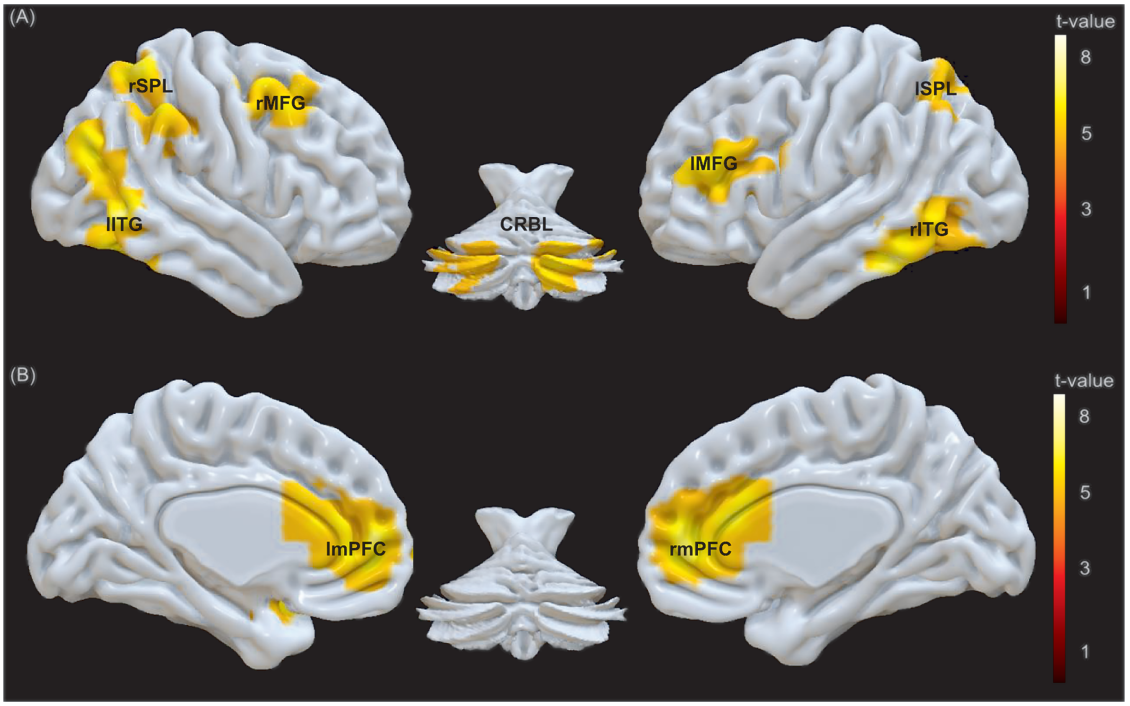

Fig. 5. Modulation of connectivity of the amygdala by action type. Co-activation of the amygdala as seed region for the contrasts (A) individual *vs* communicative (IND > COM) and (B) communicative *vs* individual (COM > IND). The threshold was set to $P < 0.05$ (FWE) at voxel level and cluster size $k > 100$. [(A) l/rITG, left/right inferior temporal gyrus; l/rSPL, left/right superior parietal lobule; l/rMFG, left/right middle frontal gyrus; CRBL, cerebellum; (B) l/rmPFC, left/right medial prefrontal cortex including peak voxels in the superior medial and orbitofrontal gyri as well as in the anterior cingulate cortex]

bility to correctly detect a second agent but was not reflected in an increased rate of FA responses. On the neural level, the right SFG was shown to be sensitive to communicative action cues, specifically, if predictions drawn from them were violated. Furthermore, neural activation in the amygdala was negatively correlated with perceptual sensitivity. Building on this, in a subsequent psychophysiological interaction analysis, we identified two distinct modes of operation. In the context of individual actions, the amygdala increased its functional connectivity with fronto-parietal areas, whereas in a context of communicative signals, the amygdala was functionally coupled to the mPFC.

While replicating the effects of IPPC on sensitivity d' and response criterion c, namely higher d' values and less conservative response criteria after communicative compared to individual actions in the behavioral study, effects commuted to non-significant trends in the fMRI study. Despite carefully controlling task difficulty and gaze behavior of participants as had been done in the behavioral study, it needs to be considered that the pre-test was performed outside of the scanner. Therefore, participants had to cope with a change in environment when performing the main part of the experiment inside the MRI scanner.

In line with our expectations, for the main effect of task *vs* baseline, we found bilateral neural activation in frontal motor areas, superior parietal, inferior temporal and visual areas, constituting an action observation network (Caspers *et al.*, 2010) and representing key regions for biological motion perception (Pavlova, 2012). Diverging from this activation map, perception of communicative actions, particularly if this communicative action is not followed by a congruently reacting agent B but Noise, led to a differential increase of neural activity in a laterally spread right SFG, a region that has been attributed to prospective memory and future planning (Barbey *et al.*, 2009; Underwood *et al.*, 2015). By incorporating predictions drawn from episodic event knowledge (Bludau *et al.*, 2014) the SFG is assumed to be particularly sensitive to the violation of predictions (Wood *et al.*, 2004). Accordingly, we find the strongest SFG activation in response to communicative actions that are not followed by an expected second agent. Contrary to our expectations, communicative actions compared to individual actions did not lead to an increased BOLD signal in the mPFC. An explanation for this might be that although only communicative actions represented signals of social consequences, a point-light agent always represented a social entity. Moreover, repeated presentation of communicative stimuli might have suppressed the neural response in the mPFC (Heleven and Van Overwalle, 2016). Eventually, it needs to be considered that the present task might not evoke any changes in mPFC activation. In comparison, by recruiting inferior temporal, superior parietal and frontal regions, individual compared to communicative actions activated a neural network similar to the task *vs* baseline contrast. Besides forming part of an action observation network and thus, realizing biological motion or action processing (Caspers *et al.*, 2010; Pavlova, 2012), dorsal fronto-parietal areas are thought to execute top–down attentional control in order to cope with high demands during early visuo-perceptual processing (Majerus *et al.*, 2018; Vossel *et al.*, 2012). In concordance with this, participants adopted a conservative response strategy when being confronted with individual actions, reporting the presence of a second agent less often than after communicative actions.

Second, we investigated the interaction effects of conditions on neural activation. In accordance with the predictive coding account (Friston, 2002) and empirical findings that assume the BOLD response to diminish as a function of reduced mismatch between higher-level predictions and the actual sensory

input (Alink *et al.*, 2010; Egner *et al.*, 2010), we did not find any significant neural clusters in the EO *vs* NEO contrast. However, the reversed NEO *vs* EO contrast elicited increased neural activation in the left cerebellum, left FFG, right pmFG and parietal areas embracing the bilateral precunei. Here, given an outcome that contradicted the predictions about the presence or absence of agent B, cerebellar and parietal activations are in agreement with cumulated evidence supporting the importance of cerebello-cortical contributions in the computation of error signals (Sokolov *et al.*, 2017). Likewise, activation in the left FFG and the pmFG have previously been related to incongruent contrasted to congruent pairs of stimuli (Cieslik *et al.*, 2015; Quadflieg *et al.*, 2015).

Third, in a regression analysis, we demonstrated that neural activation in the left amygdala during task contrasted to baseline negatively correlated with participant-specific sensitivity d'. Therefore, activation in the amygdala decreased with increasing perceptual ability to discriminate between Signal and Noise. In line with our expectations of neural correlates involved in higher-order computations, the amygdala has been portrayed as functional node between bottom-up driven perception and top–down predictions (Bzdok *et al.*, 2013). Additionally, evidence points toward the amygdala's role of adjusting attentional foci and motor responses in correspondence with the assigned salience and relevance of stimuli for a specific task (Adolphs, 2010). Consequently, higher involvement of the amygdala might indicate difficulties in coordinating stimulus-oriented and stimulus-independent processing, which results in a reduced ability to discriminate between Signal and Noise. Concerning the second regression analysis, we did not find any neural correlates of criterion c values. Here, in light of the small sample size of $N = 27$, the method used might not have provided enough statistical power to reveal a small correlational effect (Cremers *et al.*, 2017).

By means of a psychophysiological interaction analysis, we investigated the functional connectivity of the amygdala. In the context of individual compared to communicative actions, the amygdala was more functionally coupled to a fronto-parietal network that had already been observed during the task > baseline contrast and the main effect of individual *vs* communicative actions and that is known to emerge in tasks that require executive control to enable action processing and biological motion perception (Caspers *et al.*, 2010; Rottschy *et al.*, 2012; Pavlova, 2012). In conformity with this finding, the amygdala also co-activated with the inferior temporal gyri, which are thought to be important in early visual motion processing contributing to the recognition of meaningful figures (Peuskens *et al.*, 2005; Jastorff and Orban, 2009). Additional co-activation was found in the cerebellum, an area known to contribute to inhibitory motor control (Picazio and Koch, 2015). Conversely, in the context of communicative actions, the amygdala was coupled to the left Tp as well as extensive regions in the superior medial gyrus, orbitofrontal gyrus and anterior cingulate cortex, which we will refer to as mPFC. Both the left Tp and the mPFC have been deemed critical for complex social inference (Amodio and Frith, 2006; Cohn *et al.*, 2015; Yang *et al.*, 2015). Thus, although both communicative and individual point-light actors create a social context, only during communicative trials, the amygdala increases its functional coupling to brain areas implicated in mentalizing. In light of the fast and automatic nature of amygdala functioning in social cognition (Satpute and Lieberman, 2006), our findings indicate that the amygdala might play a calibrating role in adapting to the specific social context either being predictive or non-predictive. Given the negative relationship of sensitivity d' and neural activation in the amygdala, the psychophysiological interaction analysis shows two antithetical modes of perceptual decrement. In a context of individual actions, high joint activation of fronto-parietal regions, the inferior temporal gyri and thalami potentially reflects high-task demands whereas in a context of communicative actions, the amygdala may promote the integration of mentalizing-based computations.

Conclusions

Taken together, our findings indicate a neural representation of predictions drawn from communicative actions. More specifically, we showed that the right SFG and an action observation network were responsive to the violation of predictions. Moreover, reduced activation in the action observation network after communicative actions might further reflect a decreased need for executive control in order to meet the perceptual demands of the task. Amygdala signaling, however, was associated with decreased overall perceptual sensitivity. Pivotally, in the context of communicative actions, the amygdala increased its functional coupling to mPFC, an area known to be involved in mentalizing processes. Future studies shall deepen our understanding of IPPC by manipulating the probability of FA responses, namely the perception of the so-called 'Bayesian ghost' (Manera *et al.*, 2011c), while controlling for confounding effects due to a change in the experimental setting.

Supplementary data

Supplementary data are available at *SCAN* online.

Conflict of interest. None declared.

Funding

L.S. was supported by a grant for an Independent Max Planck Research Group; C.B. was supported by the European Research Council under the European Union's Seventh Framework Programme (FP/2007-2013)/European Research Council Grant Agreement.

References

Adolphs, R. (2010). What does the amygdala contribute to social cognition. *Annals of the New York Academy of Sciences*, **1191**, 42–61.

Alink, A., Schwiedrzik, C.M., Kohler, A., *et al.* (2010). Stimulus predictability reduces responses in primary visual cortex. *Journal of Neuroscience*, **30**, 2960–6.

Amodio, D.M., Frith, C.D. (2006). Meeting of minds: the medial frontal cortex and social cognition. *Nature Reviews Neuroscience*, **7**, 268–77.

Barbey, A.K., Krueger, F., Grafman, J. (2009). Structured event complexes in the medial prefrontal cortex support counterfactual representations for future planning. *Philosophical Transactions of the Royal Society, B: Biological Sciences*, **364**, 1291–300.

Becchio, C., Manera, V., Sartori, L., *et al.* (2012). Grasping intentions: from thought experiments to empirical evidence. *Frontiers in Human Neuroscience*, **6**, 117.

Bludau, S., Eickhoff, S.B., Mohlberg, H., *et al.* (2014). Cytoarchitecture, probability maps and functions of the human frontal pole. *NeuroImage*, **93**(Pt 2), 260–75.

Brainard, D.H. (1997). The psychophysics toolbox. *Spatial Vision*, **10**, 433–6.

Brett, M., Anton, J., Valabregue, R., *et al.* (2002). Region of interest analysis using an SPM toolbox. In: *8th International Conference on Functional Mapping of the Human Brain, Sendai, Japan, 2–6 June 2002*[Abstract] available on CD-ROM in NeuroImage, Vol 16, No 2.

Burr, D.C., Neri, P., Morrone, M.C. (1998). Seeing biological motion. *Nature*, **395**, 894–6.

Bzdok, D., Laird, A.R., Zilles, K., *et al.* (2013). An investigation of the structural, connectional, and functional subspecialization in the human amygdala. *Human Brain Mapping*, **34**, 3247–66.

Caballero-Gaudes, C., Reynolds, R.C. (2017). Methods for cleaning the BOLD fMRI signal. *NeuroImage*, **154**, 128–49.

Caspers, S., Zilles, K., Laird, A.R., *et al.* (2010). ALE meta-analysis of action observation and imitation in the human brain. *NeuroImage*, **50**, 1148–67.

Cieslik, E.C., Mueller, V.I., Eickhoff, C.R., *et al.* (2015). Three key regions for supervisory attentional control: evidence from neuroimaging meta-analyses. *Neuroscience and Biobehavioral Reviews*, **48**, 22–34.

Cohn, M., St-Laurent, M., Barnett, A., *et al.* (2015). Social inference deficits in temporal lobe epilepsy and lobectomy: risk factors and neural substrates. *Social Cognitive and Affective Neuroscience*, **10**, 636–44.

Cremers, H.R., Wager, T.D., Yarkoni, T., *et al.* (2017). The relation between statistical power and inference in fMRI. *PLoS One*, **12**, e0184923.

Egner, T., Monti, J.M., Summerfield, C. (2010). Expectation and surprise determine neural population responses in the ventral visual stream. *Journal of Neuroscience*, **30**, 16601–16608.

Eickhoff, S.B., Stephan, K.E., Mohlberg, H., *et al.* (2005). A new SPM toolbox for combining probabilistic cytoarchitectonic maps and functional imaging data. *NeuroImage*, **25**, 1325–35.

Friston, K. (2002). Functional integration and inference in the brain. *Progress in Neurobiology*, **68**, 113–43.

Heleven, E., Van Overwalle, F. (2016). The person within: memory codes for persons and traits using fMRI repetition suppression. *Social Cognitive and Affective Neuroscience*, **11**, 159–71.

Henson, R. (2007). Efficient experimental design for fMRI. In: Penny, W., Friston, K., Ashburner, J., *et al.*, editors. *Statistical Parametric Mapping: The Analysis of Functional Brain Images*, London: Elsevier, 193–210.

Jastorff, J., Orban, G.A. (2009). Human functional magnetic resonance imaging reveals separation and integration of shape and motion cues in biological motion processing. *Journal of Neuroscience*, **29**, 7315–29.

van Kemenade, B.M., Muggleton, N., Walsh, V., *et al.* (2012). Effects of TMS over premotor and superior temporal cortices on biological motion perception. *Journal of Cognitive Neuroscience*, **24**, 896–904.

Kiebel, S., Holmes, A. (2004). The general linear model. In: Frackowiak, K., Friston, K., Frith, C., *et al.*, editors. *Human Brain Function 2*, London: Elsevier, 725–60.

Kleiner, M., Brainard, D., Pelli, D., *et al.* (2007). What's new in psychtoolbox-3. *Perception*, **36**, 1–16.

Lakens, D. (2013). Calculating and reporting effect sizes to facilitate cumulative science: a practical primer for t-tests and ANOVAs. *Frontiers in Psychology*, **4**, 863.

von der Lühe, T., Manera, V., Barisic, I., *et al.* (2016). Interpersonal predictive coding, not action perception, is impaired in autism. *Philosophical Transactions of the Royal Society of London. Series B, Biological Sciences*, **371**, 20150373.

Majerus, S., Péters, F., Bouffier, M., *et al.* (2018). The dorsal attention network reflects both encoding load and top–down control during working memory. *Journal of Cognitive Neuroscience*, **30**, 144–59.

Manera, V., Becchio, C., Cavallo, A., *et al.* (2011a). Cooperation or competition? Discriminating between social intentions by observing prehensile movements. *Experimental Brain Research*, **211**, 547–56.

Manera, V., Becchio, C., Schouten, B., *et al.* (2011b). Communicative interactions improve visual detection of biological motion. *PLoS One*, **6**, e14594.

Manera, V., Del Giudice, M., Bara, B.G., et al. (2011c). The second-agent effect: communicative gestures increase the likelihood of perceiving a second agent. *PLoS One*, **6**, e22650

Manera, V., Schouten, B., Becchio, C., *et al.* (2010). Inferring intentions from biological motion: a stimulus set of point-light communicative interactions. *Behavior Research Methods*, **42**, 168–78.

Manera, V., Schouten, B., Verfaillie, K., *et al.* (2013). Time will show: real time predictions during interpersonal action perception. *PLoS One*, **8**, e54949.

Marsh, K.L., Richardson, M.J., Schmidt, R.C. (2009). Social connection through joint action and interpersonal coordination. *Topics in Cognitive Science*, **1**, 320–39.

McLaren, D.G., Ries, M.L., Xu, G., *et al.* (2012). A generalized form of context-dependent psychophysiological interactions (gPPI): a comparison to standard approaches. *NeuroImage*, **61**, 1277–86.

Mueller-Putz, G., Scherer, R., Brunner, C., *et al.* (2008). Better than random: a closer look on BCI results. *International Journal of Bioelectromagnetism*, **10**, 52–5.

Neri, P., Luu, J.Y., Levi, D.M. (2006). Meaningful interactions can enhance visual discrimination of human agents. *Nature Neuroscience*, **9**, 1186–92.

Okruszek, Ł., P, A., Wysokiński, A., *et al.* (2017). The second agent effect: interpersonal predictive coding in people with schizophrenia. *Social Neuroscience*, 1–6.

Oldfield, R.C. (1971). The assessment and analysis of handedness: the Edinburgh inventory. *Neuropsychologia*, **9**, 97–113.

Pavlova, M.A. (2012). Biological motion processing as a hallmark of social cognition. *Cerebral Cortex*, **22**, 981–95.

Peuskens, H., Vanrie, J., Verfaillie, K., *et al.* (2005). Specificity of regions processing biological motion. *European Journal of Neuroscience*, **21**, 2864–75.

van Pelt, S., Heil, L., Kwisthout, J., *et al.* (2016). Beta- and gamma-band activity reflect predictive coding in the processing of causal events. *Social Cognitive and Affective Neuroscience*, **11**, 973–80.

Picazio, S., Koch, G. (2015). Is motor inhibition mediated by cerebello–cortical interactions. *Cerebellum*, **14**, 47–9.

Quadflieg, S., Gentile, F., Rossion, B. (2015). The neural basis of perceiving person interactions. *Cortex*, **70**, 5–20.

Rorden, C., Brett, M. (2000). Stereotaxic display of brain lesions. *Behavioural Neurology*, **12**, 191–200.

Rottschy, C., Langner, R., Dogan, I., *et al.* (2012). Modelling neural correlates of working memory: a coordinate-based meta-analysis. *NeuroImage*, **60**, 830–46.

Sapey-Triomphe, L.-A., Centelles, L., Roth, M., *et al.* (2016). Deciphering human motion to discriminate social interactions: a developmental neuroimaging study. *Social Cognitive and Affective Neuroscience*, **12**, 340–51.

Satpute, A.B., Lieberman, M.D. (2006). Integrating automatic and controlled processes into neurocognitive models of social cognition. *Brain Research*, **1079**, 86–97.

Saygin, A.P., Wilson, S.M., Hagler, D.J., *et al.* (2004). Point-light biological motion perception activates human premotor cortex. *Journal of Neuroscience*, **24**, 6181–8.

Sokolov, A.A., Miall, R.C., Ivry, R.B. (2017). The cerebellum: adaptive prediction for movement and cognition. *Trends in Cognitive Sciences*, **21**, 313–32.

Stanislaw, H., Todorov, N. (1999). Calculation of signal detection theory measures. *Behavior Research Methods, Instruments, & Computers*, **31**, 137–49.

Underwood, A.G., Guynn, M.J., Cohen, A.-L. (2015). The future orientation of past memory: the role of BA 10 in prospective and retrospective retrieval modes. *Frontiers in Human Neuroscience*, **9**, 668.

Vossel, S., Weidner, R., Driver, J., *et al.* (2012). Deconstructing the architecture of dorsal and ventral attention systems with dynamic causal modeling. *The Journal of Neuroscience*, **32**, 10637–10648.

Wood, J.N., Knutson, K.M., Grafman, J. (2004). Psychological structure and neural correlates of event knowledge. *Cerebral Cortex*, **15**, 1155–61.

Yang, D.Y.-J., Rosenblau, G., Keifer, C., *et al.* (2015). An integrative neural model of social perception, action observation, and theory of mind. *Neuroscience and Biobehavioral Reviews*, **51**, 263–75.

Yarkoni, T., Poldrack, R.A., Nichols, T.E., *et al.* (2011). Large-scale automated synthesis of human functional neuroimaging data. *Nature Methods*, **8**, 665–70.